Hindawi Publishing Corporation
International Journal of Polymer Science
Volume 2016, Article ID 2198506, 7 pages
http://dx.doi.org/10.1155/2016/2198506

Research Article

Use of Oxalic-Acid-Modified Stellerite for Improving the Filter Capability of $PM_{2.5}$ of Paper Composed of Bamboo Residues

Hua Chen,[1,2,3] Jian Lou,[1] Fei Yang,[4] Jia-nan Zhou,[1] Yan Zhang,[1] and Huabo Yao[1]

[1]*Zhejiang Provincial Key Lab for Chem & Bio Processing Technology of Farm Product, Key Laboratory of Recycling and Eco-Treatment of Waste Biomass of Zhejiang Province, Zhejiang University of Science and Technology, Hangzhou 310023, China*
[2]*Key Laboratory of Pulp and Paper Science & Technology of Ministry of Education of China, Qilu University of Technology, Jinan 250353, China*
[3]*Zhejiang Yongtai Paper Co. Ltd, Hangzhou 311421, China*
[4]*State Key Lab of Pulp and Paper Engineering, South China University of Technology, Guangzhou 510640, China*

Correspondence should be addressed to Fei Yang; yangfei@scut.edu.cn

Received 5 October 2016; Accepted 21 November 2016

Academic Editor: Weifeng Zhao

In this study, pulping conditions for kraft pulping of bamboo residues were investigated, predominantly focusing on cooking temperature and time during pulping. Oxalic acid and cationic starch were used for the modification of natural stellerite, and the use of modified stellerite for preparing filter paper for $PM_{2.5}$ filtration was investigated. The optimal pulping technology of bamboo residues was established based on the following experimental parameters: liquor ratio of 1 : 5.5, cooking temperature of 160°C, and a holding time of 2 h. Modification by oxalic acid resulted in the promotion of pore formation at the stellerite surfaces and induced the microscopic changes. Nevertheless, paper strength remained practically unchanged after the addition of fillers, indicating that the cationic starch preblend method is a promising technique for papermaking because it enhances the strength properties of paper. With the variation in the addition of modified stellerite from 3 to 15%, while simultaneously maintaining the basis weight constant at 60 gm^{-2}, the filtration efficiency of paper sheets first increased and then decreased later; thus the optimum stellerite content was found to be 9%. Filtration efficiency was suggested to be affected by gas flowing velocity.

1. Introduction

With the economic development of China as well as the growth of its transportation industry, air pollution is becoming more serious in recent years. Several contaminants and pollutants can be adsorbed on the particles suspended in the atmosphere and enter the body via respiration.

Most studies have reported that $PM_{2.5}$ (particles with an aerodynamic diameter of 2.5 μm or less) [1] with small average particles size, large-scale impact, and high specific surface area can enter the human respiratory system and even penetrate through the lung cells into blood circulation, posing serious hazards to human health [2], including asthma [3] and bronchitis [4]. More importantly studies have increasingly reported that $PM_{2.5}$ possibly stimulates the mutation of the p53 gene in nasopharyngeal epithelial cells and plays an important role in the carcinogenesis of oral tissues [5]. According to the American Cancer Society, an 8% increase in cancer mortality for every 10 μgm^{-3} increase in $PM_{2.5}$ consistency for city population has been observed.

On the other hand, China has the richest resources of bamboo in the world, where 33,000 km^2 or 3% of the country's total forest area is occupied by bamboo [6]. With the development of the bamboo industry, a large number of residues are produced, and the utilization of these bamboo residues is not greater than 10%, where its collecting and treatment has noticed by people [7].

Both domestic and international studies have indicated that fiber filter material exhibits several advantages, such as mass production, low cost, high surface area, porous nature, and good flexibility [8–12]. The main raw materials used for filter material for high-efficiency $PM_{2.5}$ capture include natural plant, synthetic fiber, glass, ceramic, and metal fibers.

Table 1: Cooking process.

Sample	Extension	Cooking temperature (°C)	Cooking time (h)
BR	Bamboo residue	—	—
P1	Pulp 1	150	1.5
P2	Pulp 2	150	2.0
P3	Pulp 3	150	2.5
P4	Pulp 4	160	1.5
P5	Pulp 5	160	2.0
P6	Pulp 6	160	2.5

Natural plant fiber, such as bamboo residues, is probably the most promising one among various $PM_{2.5}$ filter materials, attributed to its wide spread sources, low cost, and excellent reprocessing performance.

Zeolite is a type of aqueous silicoaluminate mineral with excellent adsorption characteristics. Porous zeolites have been widely used in catalysis, adsorption, and separation attributed to their open frameworks, high surface areas, and ordered pore structures [13–15]. Nevertheless, few studies have been reported on natural zeolite, despite its low cost and abundant storage [16].

In this study, the effect of filter paper made from bamboo residue and oxalic-acid-modified stellerite on $PM_{2.5}$ filtration was comprehensively investigated. Factors affecting pulping and the use of stellerite were also investigated.

2. Experimental

2.1. Materials

2.1.1. Raw Materials. Stellerite was purchased from Jinshansida Co., Ltd. (Guilin, China). Oxalic acid, sodium hydroxide (NaOH), and sodium sulfide nonahydrate ($Na_2S{\cdot}9H_2O$) with purities of 96% were supplied by Linfeng Chemical Co., Ltd. (Shanghai, China). Cationic starch with a substitution degree of 0.028 was purchased from Hengfeng Chemical Co., Ltd. (Zhejiang, China). Bamboo *(Bambusa rigida species)* residue was provided by a bamboo products company (Anji, China). The residue exhibited the following average characteristics: 49.96% cellulose, 22.88% total lignin, and 17.97% hemicelluloses.

2.1.2. Pulping and Beating. First, bamboo residue (abbreviated as BR) was crushed and screened through a mesh with a size of 160. According to ISO 287-1985 standard, its moisture content was determined to be 12.27%. Pulping was conducted by the kraft pulping method with a liquor ratio of 1 : 5.5, active alkali of 30%, and a sulfureted degree of 30%. Samples were referred to as P1, P2, P3, P4, P5, and P6 according to the cooking process as shown in Table 1.

Filtration and washing were conducted after pulping. Finally, the pulp was refined to 30°SR using a TD7 Refiner (TD7-PFI, SUST, Shanxi, China).

2.1.3. Modification of Stellerite. Stellerite was obtained from Jinshansida Co., Ltd. (Guangxi, China). First, stellerite was repeatedly washed using distilled water for removing some impurity ions, and this was followed by dehydration in an oven box at 100°C for 12 h. Second, stellerite (7.5 g) was added into a round flask containing aqueous solution of oxalic acid (150 mL, 1.0 $molL^{-1}$). Third, the reaction temperature was maintained constant at 85°C for 5 h under stirring. Next, the solid liquid mixture was filtered, and stellerite was washed with distilled water. Further, a $AgNO_3$ test was performed to ensure the absence of remaining Cl^- ions in stellerite. After grinding, stellerite was calcined at 105°C for 12 h.

2.1.4. Capping of Cationic Starch Preblend. First, distilled water (400 mL) and cationic starch (20 g) were added together in a 500-mL four-necked-round-bottom flask; and the resulting slurry was stirred to ensure sufficient mixing. Second, modified stellerite (20 g) was added to the slurry, and after stirring for 25 min at 90°C, it was dried at 95°C for 12 h. Finally, the mixture was ground into a powder, and cationic-starch-capped modified stellerite was prepared by the preblend method, with a mass ratio of 1 : 1 for cationic starch and modified stellerite.

2.1.5. Preparation of Hand Sheets and Testing. First, the beaten pulp was diluted to a consistency of 1.2% using distilled water, followed by disintegration using a standard disintegrator at 20,000 revolutions until all fiber bundles were dispersed. Second, cationic-starch-capped modified stellerite was added under stirring at 3000 revolutions for 1 min, where the concentration of the added fillers was maintained constant at 3, 6, 9, 12, and 15% (based on oven-dry pulp mass). Hand sheets with a target basis weight of 60 gm^{-2} were prepared using the ZBJ1-B Automatic Sheet Former System (SUST, Shanxi, China) according to TAPPI T 205 (TAPPI Test Methods, 2002), with the exception that the pressure utilized for wet sheet pressing was controlled at 200 kPa, followed by drying at 102°C using a Formax 12″ Drum Dryer (Thwing-Albert Instrument, USA). The hand sheets were conditioned under a controlled environment (temperature of 23 ± 1°C and relative humidity of 50 ± 1%) before analysis.

The tensile index and air permeability of hand sheets were determined according to the relevant TAPPI Standards. The tensile index of the paper sheets was determined using a WZL-300B Tensile Strength Tester (Qitongboke, China), and air permeability was tested using an Air Permeance Tester (Messmer Instruments Ltd., Testing Machines Inc., USA). The ash content of the fibers was measured according to ISO 2144:1997 method, and the ash content of the pulp and paper sheets was determined according to TAPPI T 413 om-85 (1985) standards. The retention efficiency of the fillers was calculated by using

$$R = \frac{(A - B) \cdot (1 - L - C)}{(L - B) \cdot (1 - A - C)} \times 100\%. \quad (1)$$

Here, A, B, and L represent the ash content of the paper sheets, fiber, and pulp, respectively, and C represents the loss on ignition of stellerite.

Table 2: Pore structure analysis of fibers and stellerite.

Sample	Specific surface area (S_{BET}, m^2g^{-1})	Pore volume ($V_{t\text{-plot}}$, cm^3g^{-1})	Pore size (D_{BET}, nm)	Yield (%)
P1	0.0064 ± 0.0001	0.000126 ± 0.000003	2941.4 ± 76.48	35.46 ± 0.85
P2	0.0316 ± 0.0001	0.000169 ± 0.000007	714.2 ± 14.99	38.19 ± 0.99
P3	0.0687 ± 0.0002	0.000269 ± 0.000010	405.1 ± 10.94	39.72 ± 1.23
P4	0.0753 ± 0.0005	0.000322 ± 0.000009	218.5 ± 5.244	40.98 ± 0.98
P5	0.0932 ± 0.0007	0.000358 ± 0.000012	89.4 ± 1.699	42.91 ± 1.03
P6	0.0417 ± 0.0008	0.000125 ± 0.000004	120.2 ± 3.366	36.77 ± 1.02
Natural stellerite	2.2179 ± 0.0581	0.000487 ± 0.000012	8.0 ± 0.152	—
Modified stellerite	108.8327 ± 2.1921	0.051550 ± 0.001288	1.9 ± 0.034	91.41 ± 2.01

Filtration efficiencies of various hand sheets were investigated using TSI-8130 Automated Filter Tester (TSI Company, USA). The 0.3 μm NaCl particle was used as the filtration simulation model (adjusted flow of 32 $Lmin^{-1}$).

2.1.6. Determination of Pore Distribution. A pore size distribution detector ASAP2010M (Micromeritics, USA) was used for the structural analyses of fiber pores. High-purity N_2 was used as the adsorbate, and the adsorption–desorption of high-purity N_2 was determined at 77 K in a liquid nitrogen trap by a static volumetric method.

2.1.7. Fourier Transform Infrared Spectroscopy Analysis. Fourier transform infrared (FTIR) spectroscopy analysis of the samples was conducted in the transmission mode by macrotechniques (13 mmΦ pellet; ca. 1.5 mg sample with 350 mg KBr). The spectra were recorded using a Nexus Vector spectrometer (Nexus 670, Thermo Nicolet Company, USA) under the following specifications: Apodization: triangular; detector: DTGS/KBr; regulation: 4 cm^{-1}; and number of scans: 32.

2.1.8. X-Ray Diffraction Analysis. The X-ray powder diffraction (XRD) patterns of the samples were recorded on a Bruker D8 Advance XRD instrument (step size of 0.02° with 17.7 s per step). A Generator with 40 kV and a current of 40 mA were employed as sources for CuKα radiation.

The crystallinity index was calculated from the relative intensities of the diffraction peaks [17] as follows:

$$a = \frac{I_{020}}{(I_{020} + I_{am})} \times 100\%. \quad (2)$$

Here, I_{020} represents the intensity ($2\theta \approx 22.5^\circ$) of the peak belonging to the {020}, which contributes to the strength of the crystalline region, and I_{am} represents the intensity ($2\theta \approx 18^\circ$) between the {020} and {110}, which represents the intensity of the amorphous region.

2.1.9. Scanning Electron Microscopy Analysis. Morphologies of the hand sheet surfaces were examined by scanning electron microscopy (SEM, JSM-IT300, JEOL, Japan) operating at an accelerating voltage of 15 kV. Before observation, the samples were coated with gold using a vacuum sputter-coater.

All experiments were conducted in triplicate with a relative standard deviation (RSD) of approximately 5%.

3. Results and Discussion

3.1. Pore Structure Analysis of Fibers and Stellerite. Table 2 lists the results obtained from the pore structural analysis of fibers and stellerite. The results indicated that, with increasing cooking degree, surface area and pore volume became greater than the initial volume. Moreover, pore size significantly decreased, indicative of the generation of abundant micropores and mesopores. At this stage, the pulping yield increased because of the reduction in the discharge rate during filtration after cooking. However, cooking for a long time resulted in overcooking, leading to a decrease of surface area and the destruction of the fiber porous structure. Moreover, pulping yield also decreased during overcooking, attributed to the massive reduction of fines in washing process. Thus, the optimal pulping conditions were as follows: cooking temperature of 160°C and a holding time of 2 h (sample P5).

With respect to the oxalic-acid-modified stellerite, specific surface area (S_{BET}) for natural stellerite was 2.2179 $m^2\,g^{-1}$; in contrast, for the sample treated with 1.0 mol L^{-1} oxalic acid, S_{BET} was 108.8327 $m^2\,g^{-1}$ (increase by 49 times). In particular, pore size (D_{BET}) was also significantly less than that observed for natural stellerite, indicating that a microporous structure was formed. Moreover, the modification yield was 91.41%, attributed to the removal of impurities and loss during washing.

3.2. Functional Group Analysis of Different Samples. Figure 1 shows the FTIR spectra of samples BR, P1, P2, P3, P4, P5, and P6. The peak observed at 3447 cm^{-1} is attributed to the hydroxylgroups (OH) in the fibers; it is a band characteristic of cellulose [18]. The peak observed at 2960 cm^{-1} is attributed to the C–H absorption. The strong band observed at 1642 cm^{-1} is attributed to the vibration of absorbed water molecules in the noncrystalline region of cellulose. The band observed at 1511 cm^{-1} is attributed to the vibration of the aromatic ring of lignin, and the peak observed at 1735 cm^{-1} is ascribed to the C=O stretching vibration of acetyl and carboxyl of hemicellulose [19]. The comparison of the different spectra indicated that, with increasing cooking degree, the cellulose characteristics of spectra were more apparent,

Table 3: Effect of the variation of stellerite content on filter performance*.

Dosage of stellerite (%)	0	3	6	9	12	15
Filtration efficiency (%)	59.3 ± 2.1	72.5 ± 1.9	74.1 ± 2.3	78.4 ± 2.5	76.5 ± 2.9	75.8 ± 3.1

*Gas flowing velocity = 0.2 ms^{-1}.

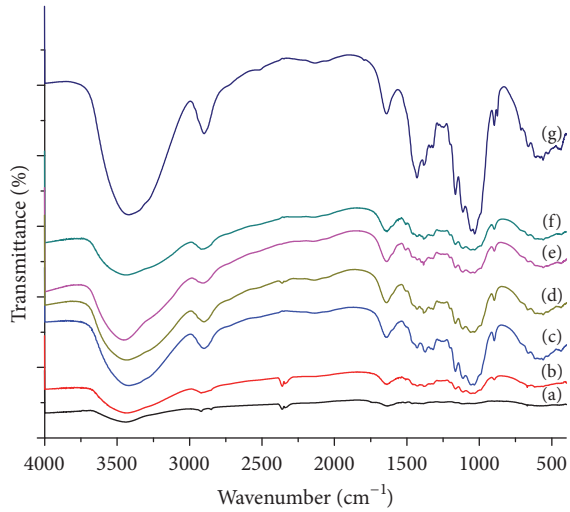

Figure 1: FTIR spectroscopy of different pulp samples: (a) BR, (b) P1, (c) P2, (d) P3, (e) P4, (f) P5, and (g) P6.

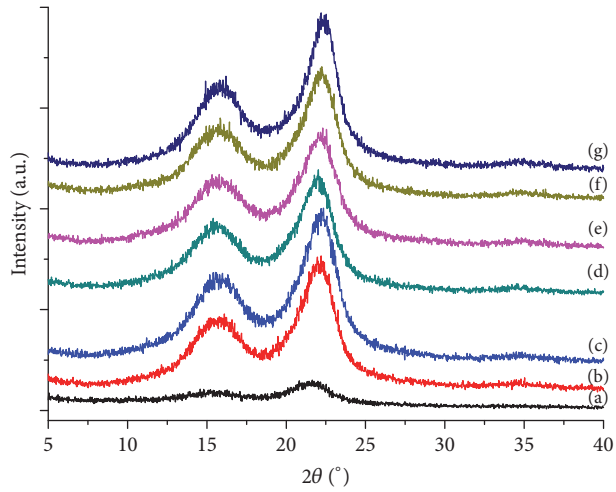

Figure 2: XRD curves of different samples: (a) BR, (b) P1, (c) P2, (d) P3, (e) P4, (f) P5, and (g) P6.

attributed to the fact that, in comparison, cellulose, lignin, and hemicellulose degrade more rapidly in the cooking process.

3.3. XRD Patterns of Fibers. Figure 2(a) shows the XRD patterns of bamboo residues, exhibiting low crystallinity (crystallinity index = 51.8%), as evidenced by their faint pattern. The crystallinity of pulp clearly increased after cooking, with the main peaks observed at 2θ of 22.5° and 18°, attributed to {020}, and the amorphous region of cellulose. Moreover, the crystallinity of P1, P2, P3, P4, P5, and P6 increased to 54.4, 55.6, 56.8, 57.2, 59.9, and 57.8%, respectively. This result is attributed to the following two reasons: the removal of disordered material in the amorphous region and the formation of new crystalline region, ascribed to the realignment of the cellulose chain caused by the penetration of water molecules into the amorphous region [19].

3.4. SEM Images of Different Samples. Figure 3 shows the SEM images of different samples, clearly displaying their surface morphology. The bamboo residues consist of piece structure, with several pits randomly distributed on the residue surface (Figure 3(a)). The bamboo fibers with complete shape and clear contours were obtained for the appropriate cooking process (P5, Figure 3(b)). Natural stellerite exhibits a clear layer structure (Figure 3(c)). Treatment with oxalic acid led to the formation of cracks on its surface, resulting in the promotion of pore formation at the stellerite surfaces and induced microscopic changes; this result is consistent with those shown in Table 2 (Figure 3(d)). Figure 3(e) shows the hand sheet without fillers, and Figure 3(f) demonstrates the distribution of granular-modified stellerite between fibers.

3.5. Ash Content and Filler Retention. Figure 4 shows the ash content and filler retention of different paper sheets. With increasing stellerite content, ash content increases, and approximately 7.2% of ash was obtained with the addition of 15% stellerite. In contrast, filler retention significantly decreases.

3.6. Tensile Indices and Air Permeability of Paper Sheets. Figure 5 shows the effects of stellerite content on the tensile indices and air permeability of the paper sheets. Compared to the control (without stellerite), the tensile index of the paper sheet with the addition of 3% stellerite indicated a 3.7% increase; however, the ash content increased from 0.14 to 1.98%. Thus, under experimental conditions employed in this study, appropriate addition of cationic-starch-preblend-modified stellerite exerted a certain positive effect on the tensile index of the paper sheet, possibly attributed to the improvement of evenness. Moreover, with increasing filler content, air permeability also increased. With the addition of 15% stellerite, the air permeability of the paper sheet increased from 3.44 to 6.62 μm Pa^{-1} s^{-1}, indicating that the porosity of the paper increased because of the addition of filler.

3.7. Filter Performance of Paper Sheets. Tables 3 and 4 summarize the filter performance of different paper sheets and the impact of gas flowing velocities. The filter performance was suggested to be affected not only by the dosage of fillers, but also by the gas flowing velocities during testing. The best performance was obtained with the addition of 9% modified

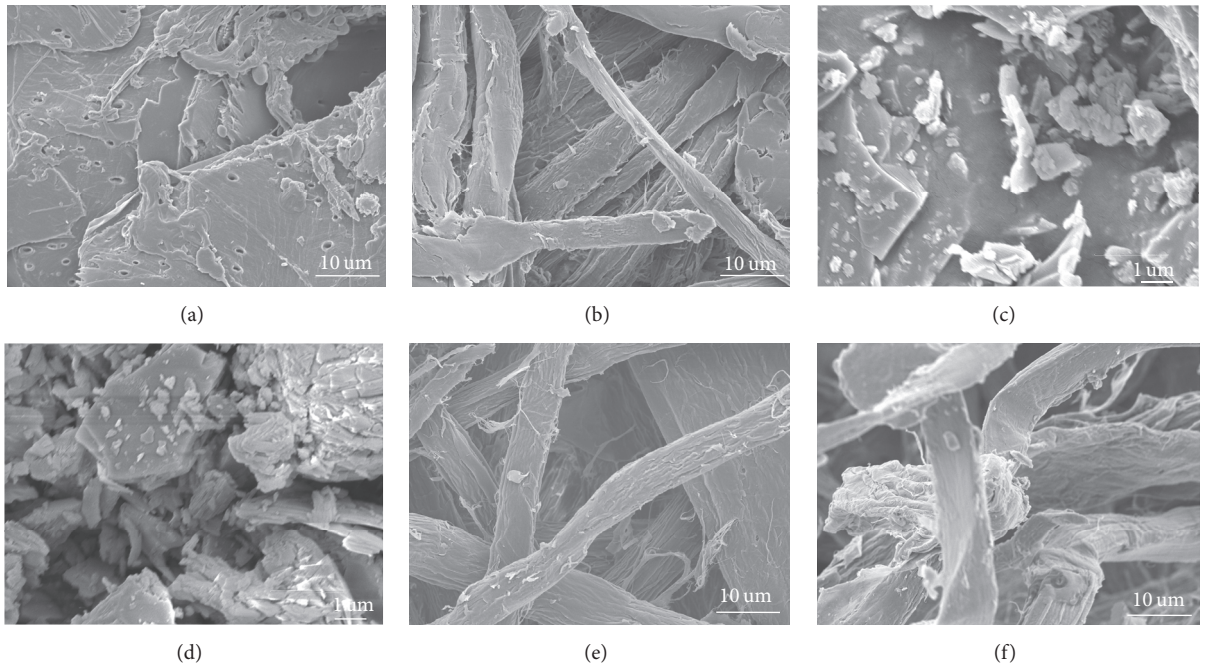

Figure 3: SEM images of different samples: (a) BR, (b) P5, (c) natural stellerite, (d) modified stellerite, (e) hand sheet composed of P5 without stellerite, and (f) hand sheet composed of P5 with modified stellerite (9%).

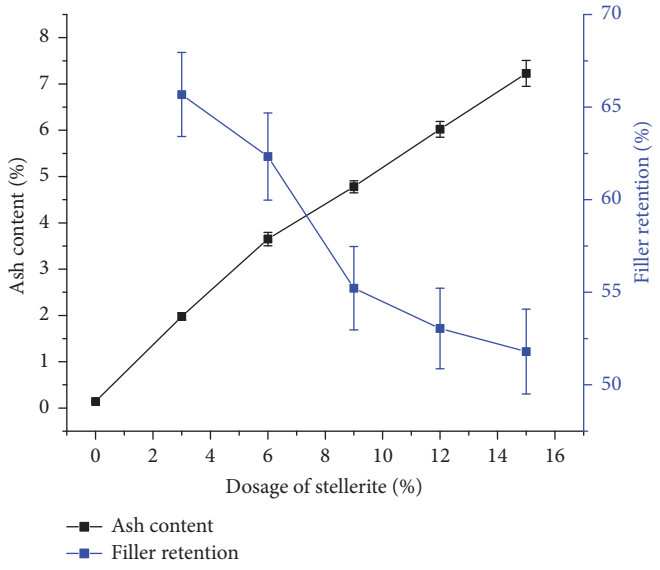

Figure 4: Ash content and filler retention of different paper sheets.

Table 4: Effect of different gas flowing velocities on filter performance*.

Gas flowing velocities (ms^{-1})	0.2	0.4	0.6	0.8
Filtration efficiency (%)	78.4 ± 2.8	69.7 ± 1.7	62.6 ± 2.5	58.2 ± 2.0

*Dosage of stellerite = 9%.

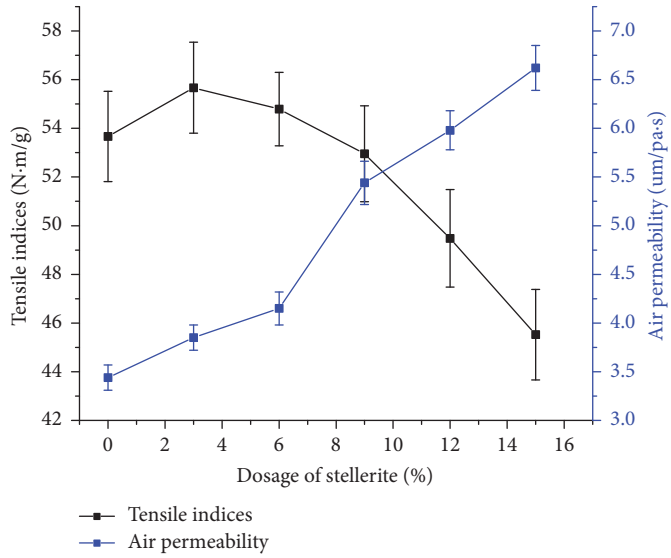

Figure 5: Tensile indices and air permeability of paper sheets.

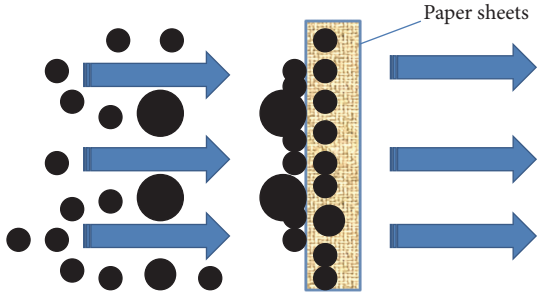

Figure 6: Filtration sketch of paper sheets.

stellerite, predominantly attributed to the fact that extremely high air permeability of paper sheets results in the decline of adsorption quantity. This result indicates the existence of an important difference between fibers and fillers in the adsorption of $PM_{2.5}$. It has been reported that micron wood fibers have low collection efficiency toward particles with the diameter from 0.4 to 0.6 μm, while they have significantly higher collection efficiency for particles with other sizes. Among these particles with the diameter of 0.01 μm, the collection efficiency of micron wood fibers can reach up to 90% [20].

In fact, the filtering process of $PM_{2.5}$ particles by plant fibers and fillers is very complex and specific to location; therefore, filter performance is affected not only by the z-direction position, but also by time. This observation is referred to as layered filtration and nonstationary filtration (see Figure 6), which will be further explored in our future study.

4. Conclusions

In this study, the following optimum cooking condition of the bamboo residues by kraft pulping was established: a liquor ratio of 1 : 5.5, a cooking temperature of 160°C, and a holding time of 2 h. Modification with oxalic acid resulted in the promotion of pore formation at the stellerite surfaces, which induced microscopic changes while simultaneously maintaining the porous structure of stellerite. The cationic starch preblend method is a promising technique for papermaking as it results in the enhanced strength of paper. The filter performance of paper sheets was significantly increased by the addition of oxalic-acid-modified stellerite. With the addition of 9% oxalic-acid-modified stellerite, the paper sheet exhibited the best filter performance (78.4%) at a gas flowing velocity of 0.2 ms^{-1}.

Competing Interests

The authors declare that they have no competing interests.

Acknowledgments

The authors greatly acknowledge the support from the Zhejiang Provincial Natural Science Foundation of China (Grant no. LY15C160002), Zhejiang Provincial Collaborative Innovation Center of Agricultural Biological Resources Biochemical Manufacturing (Grant no. 2016KF0016), and Key Laboratory of Recycling and Eco-Treatment of Waste Biomass of Zhejiang Province (Grant no. 2016REWB12).

References

[1] W.-B. Xue, F. Fu, J.-N. Wang et al., "Numerical study on the characteristics of regional transport of $PM_{2.5}$ in China," *China Environmental Science*, vol. 34, no. 6, pp. 1361–1368, 2014.

[2] B. Luo, H. Shi, L. Wang et al., "Rat lung response to $PM_{2.5}$ exposure under different cold stresses," *International Journal of Environmental Research and Public Health*, vol. 11, no. 12, pp. 12915–12926, 2014.

[3] C. Loftus, M. Yost, P. Sampson et al., "Regional PM2.5 and asthma morbidity in an agricultural community: a panel study," *Environmental Research*, vol. 136, pp. 505–512, 2015.

[4] R. Ghosh, P. Rossner, K. Honkova, M. Dostal, R. J. Sram, and I. Hertz-Picciotto, "Air pollution and childhood bronchitis: interaction with xenobiotic, immune regulatory and DNA repair genes," *Environment International*, vol. 87, pp. 94–100, 2016.

[5] L. Calderon-Garciduenas, A. Rodriguez-Alcaraz, A. Villarreal-Calderon, O. Lyght, D. Janszen, and K. T. Morgan, "Nasal epithelium as a sentinel for airborne environmental pollution," *Toxicological Sciences*, vol. 46, no. 2, pp. 352–364, 1998.

[6] J. M. O. Scurlock, D. C. Dayton, and B. Hames, "Bamboo: an overlooked biomass resource?" *Biomass and Bioenergy*, vol. 19, no. 4, pp. 229–244, 2000.

[7] M. He, Y. Zhang, Q. Hu et al., "Comparison of different pretreatment methods for bamboo residues," *Chinese Journal of Appplied Environmental Biology*, vol. 17, no. 2, pp. 232–236, 2011.

[8] J. Li, F. Gao, L. Q. Liu, and Z. Zhang, "Needleless electro-spun nanofibers used for filtration of small particles," *Express Polymer Letters*, vol. 7, no. 8, pp. 683–689, 2013.

[9] J. Li, X. Shi, F. Gao et al., "Filtration of fine particles in atmospheric aerosol with electrospinning nanofibers and its size distribution," *Science China Technological Sciences*, vol. 57, no. 2, pp. 239–243, 2014.

[10] Y. Mei, Z. Wang, and X. Li, "Improving filtration performance of electrospun nanofiber mats by a bimodal method," *Journal of Applied Polymer Science*, vol. 128, no. 2, pp. 1089–1094, 2013.

[11] J. Lang, S. Cheng, J. Li et al., "A monitoring and modeling study to investigate regional transport and characteristics of PM2.5 pollution," *Aerosol and Air Quality Research*, vol. 13, no. 3, pp. 943–956, 2013.

[12] N. Vitchuli, Q. Shi, J. Nowak, M. McCord, M. Bourham, and X. Zhang, "Electrospun ultrathin nylon fibers for protective applications," *Journal of Applied Polymer Science*, vol. 116, no. 4, pp. 2181–2187, 2010.

[13] L. Wang, C. Han, M. N. Nadagouda, and D. D. Dionysiou, "An innovative zinc oxide-coated zeolite adsorbent for removal of humic acid," *Journal of Hazardous Materials*, vol. 313, pp. 283–290, 2016.

[14] K. Guesh, C. Márquez-Álvarez, Y. Chebude, and I. Díaz, "Enhanced photocatalytic activity of supported TiO_2 by selective surface modification of zeolite Y," *Applied Surface Science*, vol. 378, pp. 473–478, 2016.

[15] P. Vinaches, J. A. B. L. R. Alves, D. M. Melo, and S. B. C. Pergher, "Raw powder glass as a silica source in the synthesis of colloidal MEL zeolite," *Materials Letters*, vol. 178, pp. 217–220, 2016.

[16] H. Chen, J. Wang, H. Wang et al., "Preparation of stellerite loading titanium dioxide photocatalyst and its catalytic performance on methyl orange," *Journal of Nanomaterials*, vol. 2015, Article ID 701589, 6 pages, 2015.

[17] Y. M. Chen, J. Q. Wan, Y. W. Ma, W. W. Wu, and Y. Wang, "Effects of pressing and drying on the cellulose crystalline degree of recycled fiber," *China Pulp & Paper Industry*, vol. 8, pp. 26–29, 2008.

[18] C. Da Silva Meireles, G. R. Filho, R. M. N. De Assunçã, M. Zeni, and K. Mello, "Blend compatibility of waste materials—cellulose acetate (from sugarcane bagasse) with polystyrene (from plastic cups): diffusion of water, FTIR, DSC, TGA, and SEM study," *Journal of Applied Polymer Science*, vol. 104, no. 2, pp. 909–914, 2007.

[19] D. L. Cheng, S. X. Jiang, and Q. S. Zhang, "The effect and mechanism of cooking on the chemical components of bamboo fibers," *Journal of Bamboo Research*, vol. 29, no. 1, pp. 50–53, 2010.

[20] X. R. Guo and P. Wang, "Simulation of steady collection efficiency of micron wood fiber pits on ultrafine particles," *Journal of Nanjing Forestry University: Natural Sciences Edition*, vol. 38, no. 3, pp. 98–102, 2014.